



26 complete *Eccaparadoxides pradoanus* thoraces from Mesones de Isuela (Murero  
27 Formation, Cambrian Series 3, Drumian). 10 injuries on 69 *E. pradoanus* thoraces from  
28 Purujosa (Murero Formation, Cambrian Series 3, Drumian) were noted. There is no  
29 evidence for laterally asymmetric predation or size selection on the trilobites in this  
30 study. Weak evidence for selection for the rear of the thorax is documented. A series of  
31 injured trilobites illustrates four stages of the healing process. Analysis of injury  
32 locations and frequency suggests that injuries to these trilobites are predatory in origin.  
33 Semilandmark analysis of previously described exoskeletons with unrepaired damage  
34 assigned to the ichnotaxon *Bicrescomanducator serratus* alongside newly collected  
35 damaged exoskeletons from Purujosa (Mansilla and Murero Formations, Stage 5 -  
36 Drumian), Mesones de Isuela (Murero Formation, Drumian), and Minas Tierga  
37 (Huérmeda Formation, Stage 4) found that shapes of biotic and abiotic breaks could not  
38 be distinguished.

39

40

## INTRODUCTION

41 Predator-prey interactions, including sub-lethal and lethal damage, have been studied  
42 using repaired exoskeletons, shells, drillholes, and broken sclerites, exemplifying the  
43 importance of predation as a potential evolutionary driver (e.g., Vermeij 1987; Kowalewski  
44 et al. 1998; Kowalewski 2002; Kelley et al. 2003). Repaired injuries preserved in different  
45 depositional environments and on skeletons of a wide variety of prey offer direct evidence of  
46 biotic interaction between predators and prey (e.g., Kowalewski 2002; Babcock 2003).  
47 Studies on repaired injuries have shown that the morphology of prey affects the frequency of  
48 repaired damages (e.g., Alexander 1986; Dietl et al. 2000; Alexander and Dietl 2001; Dietl  
49 2003a, b; Dietl and Hendricks 2006; Harper et al. 2009), and morphological characters such  
50 as spiny shells and reduced aperture sizes are adaptations in response to predation pressure

51 (Vermeij 1977, 1987; Kelley 1989; Klompmaker and Kelley 2015). Potential physical  
52 defensive adaptations in trilobites include growth to large size (e.g., *Paradoxides davidis* –  
53 Bergström and Levi-Setti 1978), development of additional spines and lengthening existing  
54 spines (e.g., *Psychopyge elegans* – Morzadec 1988), and thickening of the exoskeleton.  
55 Behavioral defensive adaptations include enrolment (e.g., *Eccaparadoxides pradoanus* –  
56 Esteve et al. 2011, 2013), burrowing (e.g., *Symphysurus angustatus* – Fortey 1986), or  
57 infaunal habit (e.g., *Paciphacops* - Rustán et al. 2011). Finally, some trilobites occupied low  
58 oxygen environments, potentially as refugia from predation (e.g., *Elrathia kingii* – Gaines  
59 and Droser 2003). Many of these adaptations (enrolment, occupation of low oxygen  
60 environments, growth of elongated pleural spines) originated in the Cambrian, perhaps driven  
61 by predatory pressure. The sophistication of predatory behavior also increased over time,  
62 showing the importance of predator-prey escalation as an evolutionary driver (Kowalewski et  
63 al. 1998; Brett and Walker 2002; Aberhan et al. 2006).

64 Trilobites were preyed upon since the Cambrian, and have been reported in the gut  
65 contents of *Ottoia prolifica* Walcott 1911, *Sidneyia inexpectans* Walcott 1911, *Wisangocaris*  
66 *barbarahardya* Jago et al. 2016, and a *Fuxianhuia*-like arthropod (Conway Morris 1977;  
67 Bruton 1981; Zhu et al. 2004; Vannier 2012; Zacaï et al. 2015; Jago et al. 2016) as well as in  
68 coprolites (Sprinkle 1973; Conway Morris and Robison 1988; Nedin 1999; Babcock 2003,  
69 Skinner 2005; Vannier and Chen 2005; English and Babcock 2010; Daley et al. 2013;  
70 Kimmig and Strotz 2017). Such examples are only recorded in exceptional preservation  
71 fossilization events, whereas damage and repair of mineralized trilobite exoskeletons are  
72 more easily preserved (Lochman 1941; Sinclair 1947; Šnajdr 1978; Rudkin 1979; Owen  
73 1985; Babcock 1993). Trilobite abnormalities and repair have been attributed to predation,  
74 problematic moulting, genetic malfunction, parasites, and accidental damage. The predation  
75 or scavenging trace fossil taxon *Bicrescomanducator serratus* (Zamora et al. 2011) describes

76 unrepaired damage on trilobite sclerites that consists of asymmetric V- or W-shaped serrated  
77 breakage of variable length, with a first-order path that is straight, or sometimes slightly  
78 arcuate (Zamora et al. 2011; Buatois et al. 2017). This trace can be seen on trilobite  
79 exoskeletons and fragments from the Cambrian Series 3 (Drumian) Purujosa 3 section of the  
80 Murero Formation, NE Spain (Zamora et al. 2011, fig. 2), Cambrian Drumian (Marjuman)  
81 section of the Rabbitkettle Formation, SW Canada (Pratt 1998, figs. 8, 9, 10), and the  
82 Ordovician Valongo Formation in Portugal (Sá and Gutiérrez-Marco 2015, fig. 12), and is  
83 attributed to *Anomalocaris* in the Cambrian and orthoceratids in the Ordovician (Zamora et  
84 al. 2011; Sá and Gutiérrez-Marco 2015). Sá and Gutiérrez-Marco (2015) synonymized  
85 *Mandibulichnus* Zamora et al. 2011 with *Bicrescomanducator* Donovan et al. in Andrews et  
86 al. 2010, as both describe irregular asymmetric breaks which occur singularly, with the  
87 difference between the type species *Bicrescomanducator rolli* Donovan et al. in Andrews et  
88 al. 2010 and *B. serratus* being the shape of the breaks: *B. rolli* is sub-crescentic and *B.*  
89 *serratus* is serrated. Although subsequent authors have continued to use *Mandibulichnus*  
90 (e.g., Neto de Carvalho et al. 2016; Buatois et al. 2017), here we treat the differences between  
91 these bioerosion traces at the species level, and so use *Bicrescomanducator serratus*. Not all  
92 broken trilobite sclerites are caused by the action of predators or scavengers and abiotic  
93 damage in trilobites has been recognized (e.g., Webster and Hughes 1999, Webster et al.  
94 2008).

95 Injuries and abnormalities in trilobites are used to understand the repair mechanisms  
96 of exoskeletons, as reviewed in the landmark publication by Owen (1985) and subsequently  
97 by Bicknell and Paterson (2017). Trilobite abnormalities can result from injuries, teratologies  
98 and pathologies (Owen 1985). Injuries can be caused by predation, accidental damage,  
99 intraspecific competition, or damage during moulting (Owen 1985; Babcock 1993).  
100 Trilobites healed over a number of moult cycles (e.g., Šnajdr 1978; Owen 1985) that

101 followed an initial callousing and regrowth over the injury (e.g., Schoenemann et al. 2017).  
102 When attacked during the soft post-ecdysial stage, trilobite spines could wrinkle or distort  
103 (Conway Morris and Jenkins 1985), and rarely additional pleural spines grew from injured  
104 areas (Babcock 1993). Regeneration of spines is controlled by segment polarity genes  
105 (McNamara and Tuura 2011), and begins during ecdysis after the damage was sustained  
106 (Lochman 1941). Regrown spines remain shorter than original spines for a variable number  
107 of moults, likely dependent on the severity of the injury. This process is comparable to the  
108 regeneration of tail spines in *Daphnia* and crinoid arms (Murtaugh 1981; Baumiller and Gahn  
109 2012).

110 Examining repaired injuries and drillholes on exoskeletons at various locations and in  
111 different formations is important for understanding the variability of predation pressure  
112 across space and time (Harper 2016). Such data can also be used to identify stereotypy of  
113 predators targeting specific locations on prey exoskeletons or specific prey sizes (e.g.,  
114 Conway Morris and Bengtson 1994; Leighton 2001, 2011; Robson and Pratt 2007). Previous  
115 quantitative studies on repaired trilobites showed non-random distribution of repaired injuries  
116 as evidence for predator site selection (Babcock and Robison 1989; Babcock 1993, 2003).  
117 When data from Cambrian trilobites was treated statistically it was shown that most scars on  
118 trilobites were incurred on the posterior right-hand side of the thorax (Babcock 1993).

119 Using exoskeletons and broken sclerites of trilobites from three sites (Purujosa,  
120 Mesones de Isuela, and Minas Tierga) from two formations (Murero Formation and  
121 Huérmeda Formation) in the Iberian Chain, NE Spain, evidence of sub-lethal predation and  
122 broken sclerites was recorded. Repaired injuries demonstrate unequivocally damage during  
123 the life of the animal. The proportion of injured trilobites at each site, and position of repaired  
124 injuries on the exoskeletons are analyzed to provide information about causes, selection  
125 pressures, and predation intensity. The location of repaired injuries is statistically tested for

126 lateral asymmetry and anteroposterior selection. Breaks on isolated sclerites from these sites  
127 and additional specimens from the Mansilla Formation (Cambrian Series 3, Stage 5) and  
128 *Bicrescomanducator serratus* breaks from the literature are assessed using a semilandmark  
129 morphometric analysis to quantify the variance of abiotic and *B. serratus* breaks.

130

### 131 GEOGRAPHIC AND GEOLOGICAL SETTING

132 All trilobites were collected from the Iberian Chain (NE Spain), near Zaragoza (Fig.  
133 1A). Specimens from the Murero Formation (Cambrian Series 3, Drumian) were collected at  
134 two localities, the first near the village of Mesones de Isuela (Fig. 1C) and the second near  
135 Purujosa (Fig. 1D), specifically the Purujosa 3 section (2 km south of Purujosa village,  
136 Zaragoza province) inside the limits of the Moncayo Natural Park (Fig. 1D). The trilobite  
137 taxon examined for predation traces at this site, *Eccaparadoxides pradoanus* (Verneuil and  
138 Barrande in Prado et al. 1860) is found as abundant broken sclerites, together with  
139 ptychopariids in the uppermost red shales of the upper Murero Formation (Fig. 2–star). The  
140 Murero Formation at both Mesones de Isuela and Purujosa represents an offshore marine  
141 environment (Álvaro and Vennin 1997; Gámez Vintaned et al. 2009). Other biomineralized  
142 groups within the faunal assemblage include protorthacean and lingulid brachiopods,  
143 sponges, echinoderms, and agnostids (Zamora 2010; Mergl and Zamora 2012).  
144 *Eccaparadoxides* is also known from lower levels in the Purujosa 3 section, and both repaired  
145 injuries and broken sclerites have been reported (Zamora et al. 2011, fig. 1C). The Mesones  
146 de Isuela locality is an outcrop 500 m east of the M3 section (Valenzuela et al. 1990) (Fig.  
147 1C). At the Mesones de Isuela locality, the Murero Formation has been subdivided into two  
148 parts: a lower part with green shales alternating with sandy units, and an upper part with red  
149 shales. Articulated *E. pradoanus* were collected from upper section of the green shale, just

150 below the appearance of the first sandy unit, alongside numerous isolated broken sclerites of  
151 the same taxon (Fig. 2).

152 The Huérmeda Formation, Cambrian Series 2, Stage 4 (Gozalo et al. 2008) was also  
153 deposited in open marine offshore conditions (Gámez Vintaned et al. 2009). It is a  
154 monotonous succession of green-grey shales with subsidiary dolostone interbeds (Figs. 1C,  
155 2). Trilobites, mostly redlichiid taxa, are present at the base of the Huérmeda Formation (e.g.,  
156 Sdzuy 1961; Schmitz 1971; Schmidt-Thomé 1973). Beds consisting of large accumulations  
157 of isolated sclerites are found between the beds containing complete trilobites.

158

## 159 MATERIALS AND METHODS

159

### 160 Collection of trilobites

160

161 Bulk samples of trilobites were collected from all sites, and broken trilobite sclerites  
162 were collected from the Mansilla Formation (Cambrian Series 3, Stage 5) near Purujosa  
163 (Figs. 1C, 2), allowing the analysis of broken sclerites to be extended through the Cambrian  
164 Stage 4, Stage 5, and Drumian. Specimens collected from the field, studied and illustrated  
165 herein, are housed at the Museo de Ciencias Naturales de la Universidad de Zaragoza (MPZ).  
166 Additional specimens, collected from the nearby Barranco del Judio and Las Cuevas/Las  
167 Coronadas localities (Fig. 1C) and other levels at the Minas Tierga locality (Fig. 2), were  
168 examined from private collections (Supp Fig. 1) and the MPZ collections. The data from  
169 private specimens were recorded separately from field specimens in case of collection bias in  
170 private collections, however as these collectors assisted in the field for this study, collection  
171 bias in the private collection is unlikely. Measurements of trilobites and abnormalities were  
172 made using digital callipers. Specimens in private collections were measured using  
173 photographs and ImageJ.

174

175 Measurement collection and observations

176 Specimens with an equal number of thoracic spines visible on each side were used to  
177 calculate potential asymmetry in repair location, and only specimens with complete thoraces  
178 were used to calculate repair frequencies and multiple repair frequencies. Other incomplete  
179 specimens were not used for any analysis. The pygidium and cephalon were not studied for  
180 injuries as they were not always preserved. Comparative data on repaired injuries from the  
181 Wheeler Formation was obtained from Babcock (1993). Repaired injuries were identified as  
182 shortened spines with recognizable healing, either in the form of rounded edges or partially  
183 regrown distal spine tips.

184 Specimens from the northern part of the Iberian Chains are preserved slightly  
185 flattened, but still show some three-dimensional features as fragile regional deformation and  
186 carbonate interbeds prevented strong deformation. This is different from specimens from the  
187 classic Murero locality, which are more flattened. Other studies on trilobites from the  
188 northern Iberian Chains (and the same locality as specimens in this study) have shown three  
189 dimensional behaviors, such as enrolment (Esteve et al. 2011, 2013).

190

191 Statistics and calculations for repaired injuries

192 *Frequency of repairs.*— Repair frequency was calculated using the following metrics  
193 to allow direct comparison between sites:

$$F = \frac{\text{Number of repairs}}{\text{Number of animals}}$$

$$MF = \frac{\text{Number of animals with } > 1 \text{ repaired injury}}{\text{Number of animals with 1 repaired injury}}$$

$$R = \frac{\text{Number of animals with } \geq 1 \text{ repaired injury}}{\text{Number of animals}}$$

194 Metric F gives an inflated representation of the percentage of individuals damaged  
195 and subsequently repaired (Dietl et al. 2000), and metric R gives an underestimated



196 frequency of individuals repaired (Alexander and Dietl 2003). Following Alexander and Dietl  
197 (2003), both are presented to mitigate the limitations of both methods. For the Huérmeda  
198 Formation, the repair frequency was calculated using all redlichiid trilobites, and for the  
199 Murero Formation the repair frequency was calculated using *Eccaparadoxides pradoanus*.  
200 Although repair frequencies for the Wheeler Formation could not be calculated from the  
201 literature, a multiple repair frequency value, MF, was derived using data from Babcock  
202 (1993, p. 222).

203 Collecting very large sample sizes of complete or near-complete trilobites is not  
204 always possible, and this affects the uncertainty of calculated repair frequencies. We use a  
205 Bayesian Inference method to estimate the effect of sample size on repair frequencies,  
206 calculating 5th and 95th percentile confidence values. This analysis was run in R Studio (R  
207 Core Team 2017; see Supp Info 1 for code).

208 *Origin and location of repaired injuries.*— Distinguishing between accidental  
209 damage, damage due to problems during moulting, or predatory damage is a complicated task  
210 when considering the cause of repaired injuries. We propose a statistical method to estimate  
211 the likelihood of damage having occurred during moulting. For trilobites that have thoracic  
212 spines of approximately equal length and similar morphology, the likelihood that a given  
213 spine is injured due to moulting complications is expected be the same as all other spines.  
214 This would result in randomly distributed injuries on trilobite exoskeletons, assuming that  
215 injuries occurred during the holaspis phase. As segments are added at the posterior of the  
216 thorax throughout meraspid stages, individual injuries due to moulting could be more  
217 common at the anterior than at the posterior, as these segments undergo more moult stages.  
218 For species with particularly long, thin, or intricate spines, this expectation changes as such  
219 spines are more susceptible to moulting damage than others. Accidental injuries from  
220 copulation, interspecific combat, or unsuccessful predatory attacks would be more likely to

221 injure multiple adjacent spines, and so injured spines would not be randomly distributed  
222 across the thorax (Babcock 1993). The ‘stats’ package (R Core Team 2017) in R Studio was  
223 employed to do a binomial test, comparing the observed number of adjacent injured spines to  
224 the expected distribution of randomly arranged injured spines (see Supp Info 1 for code). A  
225 random distribution of injured spines would suggest that moulting was a major cause,  
226 whereas a significant number of short spines adjacent to each other supports a predatory or  
227 accidental origin of the injuries.

228         Repair frequencies at Purujosa and Mesones de Isuela were calculated, as these two  
229 sites house the same species (*Eccaparadoxides pradoanus*), and were deposited in similar  
230 environments of the same age (Cambrian Series 3, Drumian). Repair frequencies were also  
231 calculated on trilobites from Minas Tierga (Cambrian Series 2, Stage 4) as they are  
232 morphologically similar to *E. pradoanus*, from a similar environment, and geographically  
233 close to Mesones de Isuela.

234         We tested both lateral and anteroposterior selection of injury location. Lateral  
235 asymmetry was tested using a two-tailed binomial test, so that selection for either the left or  
236 right could be detected. Our null hypothesis was that there is no lateral asymmetry in injury  
237 location, so an equal distribution of injuries on the left and right sides is expected. A rejection  
238 of this hypothesis supports the existence of lateral asymmetry in injury location. A two-tailed  
239 binomial test facilitates the detection of laterally asymmetric selection for the left and right  
240 sides of the thorax. A one-sided binomial, as used in other studies (e.g., Babcock and  
241 Robison 1989; Babcock 1993, 2003) allows only detection for either the right side or the left  
242 side (which must be determined before the analysis is undertaken).

243         Anteroposterior selection for the most posterior three thoracic segments of the  
244 trilobite was also tested using a two-tailed binomial test. These three thoracic segments have  
245 posterior-pointing thoracic spines, and would have covered the anterior of the cephalon

246 during enrolment. The null hypothesis was that there was no selectivity in injury location: the  
247 probability of injuring each spine is equal. This gives an expected percentage of 18.75% of  
248 injuries occurring on the rear three thoracic segments in a thorax of 16 segments. Rejecting  
249 this null hypothesis in favour of the alternative would illustrate selection either for the front  
250 13 or rear 3 thoracic segments.

251 *Size distribution and selection.*— To test if the size distribution of trilobites was  
252 similar between the three sites and to assess whether size impacted the frequency of repaired  
253 injury frequency, a Mann-Whitney U test was undertaken using the ‘stats’ package in R  
254 Studio. The Mann-Whitney U test is a non-parametric test that determines whether the means  
255 of two independent samples are equal. In this case, if the mean lengths of injured trilobites  
256 are distinguished from the mean lengths of uninjured trilobites using a Mann-Whitney U test,  
257 a size preference for attacks can be demonstrated.

258

259 *Statistics and calculations for broken sclerites*

260 A morphometric analysis was used to quantitatively assess broken sclerites. A  
261 semilandmark analysis of sclerites collected from the Murero Formation (Drumian) the  
262 Mansilla Formation (Stage 5), the Huérmeda Formation (Stage 4), *B. serratus* from the  
263 Rabbitkettle Formation (Pratt 1998), and Middle Darriwilian Valongo Formation (Sá and  
264 Gutiérrez-Marco 2015). Semilandmarking was conducted using the Thin-Plate Spline (tps)  
265 suite (<http://life.bio.sunysb.edu/morph/index.html>). A tps file was constructed using tpsUtil64  
266 (v.1.7). The tps file was imported into tspDig2 (v.2.26), which was used to place the 80 semi-  
267 landmarks along the breaks in a counter clockwise direction. As these outlines are not closed  
268 curves, a consistent placement of semilandmark direction was needed. These points were  
269 used to populate the tps file with the semilandmark data. The tps file was imported into an R  
270 environment. The ‘geomorph’ package (Adams and Otárola-Castillo 2013) was used to

271 conduct the Procrustes Superposition and Principal Components Analysis (PCA) of the  
272 superimposed data. The Procrustes Superposition was standardized for size and orientation,  
273 and so the analysis was performed solely on the variation of the outline shapes. Note that as  
274 these breaks do not have a biologically homologous landmark, no landmarked points were  
275 produced.

276

## 277 RESULTS OF ANALYSES ON REPAIRED INJURIES

278

### 279 Description of repaired injuries

280 Injuries at a number of stages of regeneration were recognized in this study (Figs. 3, 4,  
281 Zamora et al. 2011, fig. 4). These injuries healed over multiple moult stages: after callousing  
282 and initial repair (Fig. 3A, E) the end of the spine became rounded (Fig. 3B, F). This stage  
283 was followed by a thin growth with a pointed end during the subsequent moult(s) (Fig. 3C, G,  
284 Zamora et al. 2011, fig. 4D, E). Complete, but comparably shorter spines arose in the  
285 following moults (Fig. 3D, H, Zamora et al. 2011, fig. 4A-C, F-K). In one case (Fig. 4)  
286 multiple spines grew from an injured area.

287

### 288 Frequency of repairs

289 In the Murero Formation, a record of predation is only reported from the Purujosa locality  
290 (Table 1). No evidence for sublethal predation is reported from Mesones de Isuela (Murero  
291 Formation), from any locality, or private collection of material from the Huérmeda  
292 Formation. The 5<sup>th</sup> and 95<sup>th</sup> confidence intervals suggest that even though different  
293 population sizes were considered, the repair frequencies (both R and F) are significantly  
294 different (Table 1). The multiple repair frequency in the Murero Formation (0.22) is an order  
295 of magnitude higher than the Wheeler Formation (0.04) (Table 1).

296

297

#### Origin and location of injuries

298 Injured spines are not randomly distributed on trilobite exoskeletons, instead they are found

299 adjacent to each other (Binomial test,  $n=15$ ,  $p\text{-value}<0.001$ , Table 2). Injuries on *E.*

300 *pradoanus* are found at Purujosa ( $F = 0.14$ ,  $R = 0.13$ ) but not Mesones de Isuela ( $F = 0$ ,  $R =$

301  $0$ ) (Table 1).

302 Spines are not significantly more likely to be injured on the left or right sides (two-

303 tailed binomial test,  $n=16$ ,  $p\text{-value}=1$ ) and spines on the rear three thoracic segments were

304 more likely to be injured than other segments (two-tailed binomial test,  $n=10$ ,  $p\text{-}$

305  $\text{value}=0.0045$ ) (Table 3).

306

307

#### Size distribution and selection in the Murero Formation

308 No significant size selection was detected between the injured trilobite sample (mean = 38.98

309 mm, median = 32.83 mm,  $sd = 21.81$  mm) and the non-injured sample (mean = 32.14 mm,

310 median = 30.91 mm,  $sd = 13.31$  mm) at Purujosa (Mann Whitney U test,  $W=224$ ,  $p=0.46$ ).

311 This suggests that predators in the Murero Formation did not target smaller or larger trilobites

312 at Purujosa. The size distributions of trilobites collected from the field at Purujosa, Mesones,

313 and Minas Tierga cannot be distinguished according to Mann-Whitney U tests (thoracic

314 means: Purujosa, 33.02 mm, Mesones, 32.42 mm, Minas Tierga, 41.45 mm; Mann Whitney

315 U tests: Purujosa and Mesones,  $W= 816.5$ ,  $p=0.86$ ; Purujosa and Minas Tierga,  $W = 786$ ,  $p=$

316  $0.058$ ; Mesones and Minas Tierga,  $W = 439$ ,  $p = 0.094$ , lengths of specimens plotted in Supp

317 Fig. 2), suggesting that size differences are not the cause of differences in calculated repair

318 frequencies.

319

320

#### RESULTS OF ANALYSES ON BROKEN SCLERITES

321 A biotic origin for trace fossils can be inferred if they have a distinct geometric shape,  
322 a narrow size range, and/or a non-random distribution of traces across taxa, size of prey, or  
323 location on the skeletons (Kowalewski 2002). Some broken sclerites found here are  
324 putatively of biotic origin (Figs. 5A, 6 white arrows, 7), some abiotic (Figs. 5C, 6 black  
325 arrows), and some breaks are of indeterminate origin (Fig. 5B). Semilandmark analyses  
326 describe the shape variation of the broken sclerites very effectively, as the two illustrated  
327 Principal Components explain 46.3% of the shape variation (Fig. 8). PC1 shows a change  
328 from a deep to shallow break, and PC2 shows a change from a break indented on the left side  
329 to one on the right side. Fossils that are referred to *Bicrescomanducator serratus* do not have  
330 a restricted shape variation in the Principal Coordinate (PC) space: there is a large spread of  
331 *B. serratus* specimens (red squares) across both PC1 and PC2 (Fig. 8). As specimens  
332 assigned to *B. serratus* overlap in morphospace with previously described *B. serratus*  
333 specimens (Fig. 9, red shapes: compare the points with black dots to those without), the  
334 assignment of *B. serratus* is acceptable. However, the new specimens also overlap with  
335 putative abiotic shapes (Fig. 9, blue shapes) and so a biotic origin of the new specimens  
336 cannot unambiguously be assigned.

337

338

## DISCUSSION

339

### Repaired injuries

340

341

342

343

344

345

*Complete repair of trilobite injuries?* – Trilobite injuries at a number of stages of  
repair are reported in this study (Figs 3, 4). Trilobites are thought to have had indeterminate  
growth, and so continued to moult after reaching adult morphology (Daley and Drage 2016).  
Therefore it is likely given enough time a trilobite with an injury would heal completely,  
removing all evidence that an injury occurred. Each moult stage is a stage of healing (Fig.  
10A-D) and after a number of moults, dependent on the location and severity of the injury, all

346 evidence of the injury would be removed (Fig. 10E). This has a direct implication for the  
347 comparison of repair frequencies of trilobites (and other ecdysozoans) with other groups  
348 which do not moult. The calculated repair frequency for ecdysozoans is likely an  
349 underestimate of the true frequency of injuries in the population. Larger injuries, which  
350 would require more moult stages to heal, therefore have a greater impact on the repair  
351 frequency than small injuries which would heal more quickly.

352 *Origin of injuries*—The low statistical likelihood of adjacent spines being injured by  
353 chance illustrates that injuries on *Eccaparadoxides pradoanus* likely result from predatory  
354 attacks, rather than from accidents and/or problematic moulting (Table 2). This is  
355 corroborated by the lower frequency of injuries on *E. pradoanus* from Mesones: if injuries  
356 were the result of moulting problems or another consistent behavior of the trilobites, the  
357 injury value would not vary markedly between sites. As the 95<sup>th</sup> percentile repair frequency  
358 value at Mesones is lower than the measured repair frequency at Purujosa, the smaller sample  
359 size at Mesones does not account for the difference in injury frequency between these two  
360 sites. Consequently, when using the frequency of repaired trilobite injuries as a proxy for  
361 predation on *E. pradoanus*, the ‘noise’ from non-predatory damage is likely to be minimal.  
362 This may not be the case for all trilobite injuries. Indeed Šnajdr (1978) considered moulting  
363 damage the most significant cause of injury in Bohemian paradoxidids.

364 *Comparison between sites.*— A difference in repair frequency between two sites of  
365 the same age, environment, and species of trilobite suggests a difference in predator pressure  
366 at those two sites. This may not follow when the energy of the depositional environment is  
367 significantly different (as this may affect the likelihood of accidental injuries), or where the  
368 sizes of trilobites vary significantly (as predators may preferentially attack smaller or larger  
369 animals). At all three field sites, complete trilobites have similar body plans with similar  
370 sized pleural spines on relatively large thoraces. Furthermore both the Huérmeda and Murero

371 Formations are considered to represent offshore environmental conditions, sporadically  
372 affected by storms. These similarities facilitate comparison between all three sites.

373         The repair frequency metrics (R, F, and MF) in the Huérmeda Formation (Cambrian  
374 Stage 4) are lower than the Murero Formation (Drumian), however trilobites at neither Minas  
375 Tierga (Huérmeda Formation) or Mesones de Isuela (Murero Formation) show evidence for  
376 repaired injuries. These two sites are geographically closer to each other than to Purujosa,  
377 where there is evidence for repaired injuries in the Drumian (see Figs. 1, 2; Table 1) and from  
378 other levels of the Purujosa 3 section (Table 1; Zamora et al. 2011). This suggests a  
379 geographic rather than temporal cause for the difference in predation, although the absolute  
380 distances between these sites in the Cambrian would have been different than at present as  
381 the Iberian Chains have been subjected to substantial tectonic activity. A lack of injured  
382 individuals suggests that either predation intensity on the trilobites studied was very low, or  
383 that predators were 100% efficient (Schoener 1979; Alexander 1981). Three lines of evidence  
384 support an interpretation of low predation intensity in this case: failure by predators is  
385 common; trilobites could repair even extensive damage; and trilobites of the same species at  
386 a different site show repaired injuries (Vermeij 1982; McNamara and Tuura 2011;  
387 Schoenemann et al. 2017).

388         *Selectivity in repaired damage location.*— *Eccaparadoxides pradoanus* likely  
389 enrolled as a defensive measure (Esteve et al. 2013). During enrolment, the posterior part of  
390 the thorax was located over the cephalon, an area where damage would have been more  
391 likely to be fatal (Babcock 1993). The high occurrence of damage to the posterior three  
392 segments may be the result of damage incurred during defensive enrolment. Alternatively,  
393 posterior injuries may indicate that predators attacked from the rear (Babcock 1993). The  
394 lack of anterior injuries supports the observation that posterior injuries are less lethal than  
395 anterior attacks (Babcock 1993), especially as the anterior segments were created before the



396 posterior, although the small sample size and p-value (0.0045), means this result is only  
397 tentative.

398 *Comparison between the Wheeler Formation and the Murero Formation*—There is a  
399 higher multiple repair frequency in the Murero than the Wheeler Formation (Table 1).  
400 Assuming that the data collected are directly comparable, this indicates that injured  
401 specimens were more likely to be attacked a second time in the Murero Formation than the  
402 Wheeler.

403 The data from the Murero Formation show no lateral asymmetry of injuries on  
404 Cambrian trilobites, differing from the results of previous studies where site selectivity was  
405 reported for the right side of the body (Babcock and Robison 1989; Babcock 1993, 2003),  
406 specifically in the Wheeler Formation (Babcock 1993). Differences between the Wheeler and  
407 Murero Formations including environment, paleolatitude, and taxa studied, are factors that  
408 may impact on the differences observed for site selectivity of injuries and multiple repair  
409 frequency. More studies of trilobites using large datasets and similar taxa are needed to  
410 understand variation in repair frequencies and injury location selectivity.

#### 411 Broken sclerites

412 It is often not possible to distinguish between predation and scavenging (e.g.,  
413 Babcock 1993). Similar complications occur when differentiating between abiotic and biotic  
414 breakages, as fragmentation of shapes can arise from abiotic and biotic factors (Kowalewski  
415 2002; Webster et al. 2008). While taphonomic alteration of cuticle is thought to be  
416 uncommon, trilobite cephalata often fractured sagittally along the axis of highest vertical relief  
417 (Pratt 1998; Webster and Hughes 1999; Fig. 5C). Both biotic and abiotic damage to sclerites  
418 are presented and described morphometrically here.

419 V- and W-shaped traces on broken sclerites from the Huérmeda, Mansilla and Murero  
420 Formations fit the current definition of *Bicrescomanducator serratus* and overlap in PC

421 space, but show a wide variety of shapes, sizes, and angles. The large morphological  
422 variation in *B. serratus* is problematic because the semilandmark analyses did not clearly  
423 distinguish between abiotic and biotic damage, suggesting that the species definition requires  
424 refining and that caution must be applied when assigning biotic origin. Circumstantial  
425 evidence, such as co-occurring predators or repaired predatory damage, could be used to  
426 strengthen future assignments. If a biotic origin is confirmed, breaks from the Huérmeda  
427 Formation would be the oldest known representatives of *B. serratus*.

428

429

## CONCLUSIONS

430 Based on the relative frequencies of damage in trilobites from multiple localities,  
431 repaired injuries on *Eccaparadoxides pradoanus* appear to be predatory in nature. Variation  
432 in repair frequencies between the Murero, Huérmeda, and Wheeler Formations show that  
433 predation intensity can vary even on the same species of trilobite at different sites, and  
434 between different trilobite species worldwide. Evidence for predation is present at numerous  
435 levels at Purujosa, but absent in localities of the same age that are geographically more  
436 distant, suggesting that geography may be one factor affecting predation pressure. This does  
437 not mean that predation is absent at Minas Tierga or Mesones de Isuela. The location of  
438 injuries on trilobites from Purujosa showed no significant lateral asymmetry, differing from  
439 previous reports on Cambrian trilobites (Babcock and Robison 1989; Babcock 1993, 2003).  
440 The posterior three thoracic segments were targeted more often than expected from random  
441 attacks, perhaps due to *E. pradoanus* enrolling as a defensive measure.

442 A novel approach was employed using morphometric analyses to assess and compare  
443 the shape of unrepaired damage on trilobite sclerites. While the shape variation of serrated  
444 breaks on isolated sclerites was well described using this technique, *Bicrescomanducator*

445 *serratus* traces could not be distinguished from abiotically broken sclerites, suggesting that a  
446 revision to the definition of this trace fossil taxon is needed.

447

448

#### Acknowledgments

449 We thank the Coeditor Thomas Olszewski, the Associate Editor Brian Pratt, and the  
450 two reviewers Oldřich Fatka and Alan Owen, for their thoughtful comments and editorial  
451 notes that greatly improved the manuscript. We also thank Brian Pratt and Artur Sá for  
452 providing images of *Bicrescomanducator serratus* from previous studies. We appreciate the  
453 invaluable help of Fernando Gracia and Jesus García (Zaragoza, Spain) who assisted in the  
454 field; Supratik Paul for discussions of statistics; and Luis Buatois, Gabriela Mangano, and  
455 Mark Wilson for discussions of incho taxonomy. SP was funded by a Santander Travel Award  
456 and Oxford-St Catherine's Brade-Natural Motion Scholarship, RDCB was funded by an  
457 Australian Postgraduate Award, SZ was funded by a Ramón y Cajal Grant (RYC-2012-  
458 10576) and project CGL2013-48877-P from the Spanish Ministry of Economy and  
459 Competitiveness.

460

#### 461 References

462

463 ABERHAN, M., KIESSLING, W. and FÜRSICH, F.T., 2006, Testing the role of biological  
464 interactions in the evolution of mid-Mesozoic marine benthic ecosystems:

465 *Paleobiology*, v. 32, p. 259—277.

466 ADAMS, D.C., and E. OTAROLA-CASTILLO, 2013. geomorph: an R package for the

467 collection and analysis of geometric morphometric shape data: *Methods in Ecology*

468 and *Evolution*, v. 4, p. 393—399.

- 469 ALEXANDER, R.R., 1981, Predation scars preserved in Chesterian brachiopods: probable  
470 culprits and evolutionary consequences for the articulates: *Journal of Paleontology*, v.  
471 55, p. 192—203.
- 472 ALEXANDER, R.R., 1986, Resistance to and repair of shell breakage induced by durophages  
473 in late Ordovician brachiopods, *Journal of Paleontology*, v. 60, p. 273—285.
- 474 ALEXANDER, R.R. and DIETL, G.P., 2001. Latitudinal trends in naticid predation on  
475 *Anadara ovalis* (Bruguiere, 1789) and *Divalinga quadrisulcata* (Orbigny, 1842) from  
476 New Jersey to the Florida Keys: *American Malacological Bulletin*, v. 16, p. 179—  
477 194.
- 478 ALEXANDER, R.R. and DIETL, G.P., 2003, The fossil record of shell-breaking predation  
479 on marine bivalves and gastropods, *in* Kelly, P., Kowalewski, M., and Hansen, T.A.  
480 (eds.), *Predator—Prey Interactions in the Fossil Record*, Kluwer Academic, New  
481 York, p. 141—176.
- 482 ÁLVARO, J.J. and VENNIN, E., 1997, Episodic development of Cambrian eocrinoid-sponge  
483 meadows in the Iberian Chains (NE Spain): *Facies*, v. 37, p. 49—63.
- 484 ANDREW, C., HOWE, P., PAUL, C.R.C., and DONOVAN, S.K., 2010, Fatally bitten  
485 ammonites from the lower Lias Group (Lower Jurassic) of Lyme Regis, Dorset :  
486 *Proceedings of the Yorkshire Geological Society*, v. 58, p. 81—94.
- 487 BABCOCK, L. E., 1993, Trilobite malformations and the fossil record of behavioral  
488 asymmetry: *Journal of Paleontology*, v. 67, p. 217—229.
- 489 BABCOCK, L. E., 2003, Trilobites in Paleozoic predator-prey systems, and their role in  
490 reorganization of early Paleozoic ecosystems, *in* Kelly, P., Kowalewski, M., and  
491 Hansen, T.A. (eds.), *Predator—Prey Interactions in the Fossil Record*, Kluwer  
492 Academic, New York, p. 55—92.

- 493 BABCOCK, L.E. and ROBISON, R.A., 1989, Preferences of Palaeozoic predators: *Nature*, v.  
494 337, p. 695—696.
- 495 BAUMILLER, T.K. and GAHN, F.J., 2012, Reconstructing predation pressure on crinoids:  
496 estimating arm-loss rates from regenerating arms: *Paleobiology*, v. 39, p. 40—51.
- 497 BERGSTRÖM, J. and LEVI-SETTI, R., 1978, Phenotypic variation in the Middle Cambrian  
498 trilobite *Paradoxides davidis*: *Geologica et Palaeontologica*, v. 12, p. 1—40.
- 499 BICKNELL, R.D.C and PATERSON J.R., 2017, Reappraising the early evidence of  
500 durophagy and drilling predation in the fossil record: Implications for escalation and  
501 the Cambrian Explosion: *Biological Reviews*, doi: 10.1111/brv.12365.
- 502 BRETT, C.E. and WALKER, S.E., 2002, Predators and predation in Paleozoic marine  
503 environments: *Paleontological Society Papers*, v. 8, p. 93—118.
- 504 BRUTON, D.L., 1981, The arthropod *Sidneyia inexpectans*, Middle Cambrian, Burgess  
505 Shale, British Columbia: *Philosophical Transactions of the Royal Society of London*.  
506 Series B, Biological Sciences, v. 296, p. 619—653.
- 507 BUATOIS, L.A., WISSHAK, M., WILSON, M.A. and MÁNGANO, M.G., 2017, Categories  
508 of architectural designs in trace fossils: A measure of ichnodisparity: *Earth-Science*  
509 *Reviews*, v. 164, p. 102—181.
- 510 CONWAY MORRIS, S., 1977, Fossil priapulid worms: *Special Papers in Palaeontology*, v.  
511 20, p. 1—155.
- 512 CONWAY MORRIS, S. and BENGTSON, 1994, Cambrian predators: possible evidence  
513 from boreholes: *Journal of Paleontology*, v. 68, p. 1—23.
- 514 CONWAY MORRIS, S. and JENKINS, R., 1985, Healed injuries in early Cambrian  
515 trilobites from South Australia: *Alcheringa*, v. 9, p. 167—177.

516 CONWAY MORRIS, S. and ROBISON, R.A., 1988, More soft-bodied animals and algae  
517 from the Middle Cambrian of Utah and British Columbia: University of Kansas  
518 Paleontological Contributions, v. 122, p. 1—48.

519 DALEY, A.C., and DRAGE, H.B. 2016, The fossil record of ecdysis, and trends in the  
520 moulting behavior of trilobites: *Arthropod Structure and Development*, v. 45, p. 71—  
521 96.

522 DALEY, A.C., PATERSON, J.R., EDGECOMBE, G.D., GARCIA-BELLIDO, D. C. and  
523 JAGO, J. B., 2013, New anatomical information on *Anomalocaris* from the Cambrian  
524 Emu Bay Shale of South Australia and a reassessment of its inferred predatory habits:  
525 *Palaeontology*, v. 56, p. 971—990.

526 DIETL, G.P., ALEXANDER, R.R. and BIEN, W.F., 2000, Escalation in Late Cretaceous–  
527 early Paleocene oysters (Gryphaeidae) from the Atlantic Coastal Plain: *Paleobiology*,  
528 v. 26, p. 215—237.

529 DIETL, G.P., 2003a, Interaction strength between a predator and dangerous prey:  
530 *Sinistrofulgur* predation on *Mercenaria*: *Journal of Experimental Marine Biology and*  
531 *Ecology*, v. 289, p. 287—301.

532 DIETL, G.P., 2003b, Coevolution of a marine gastropod predator and its dangerous bivalve  
533 prey: *Biological Journal of the Linnean Society*, v. 80, p. 409—436.

534 DIETL, G.P. and HENDRICKS, J.R., 2006, Crab scars reveal survival advantage of left-  
535 handed snails: *Biology Letters*, v. 2, p. 439—442.

536 ENGLISH, A.M. AND BABCOCK, L.E., 2010, Census of the Indian Springs Lagerstätte,  
537 Poleta Formation (Cambrian), western Nevada, USA: *Palaeogeography*,  
538 *Palaeoclimatology, Palaeoecology*, v. 295, p. 236—244.

539 ESTEVE, J., HUGHES, N.C. and ZAMORA, S., 2011, Purujosa trilobite assemblage and the  
540 evolution of trilobite enrolment: *Geology*, v. 39, p. 575—578.

541 ESTEVE, J., HUGHES, N.C. and ZAMORA, S., 2013, Thoracic structure and enrolment  
542 style in Middle Cambrian *Eccaparadoxides pradoanus* presages caudalization of the  
543 derived trilobite trunk: *Palaeontology*, v. 56, p. 589—601.

544 FORTEY, R., 2000, Olenid trilobites: The oldest known chemoautotrophic symbionts?:  
545 *Proceedings of the National Academy of Sciences*, v. 97, p. 6574—6578.

546 FORTEY, R.A., 1986, The type species of the Ordovician trilobite *Symphysurus*: systematics,  
547 functional morphology and terrace ridges: *Paläontologische Zeitschrift*, v. 60, p.255—  
548 275.

549 GÁMEZ VINTANED, J.A., SCHMITZ, U. AND LIÑÁN, E., 2009, Upper Vendian-lowest  
550 Ordovician sequences of the western Gondwana margin, NE Spain: *Geological*  
551 *Society, London, Special Publications*, v. 326, p. 231—244.

552 GAINES, R.R. and DROSER, M.L., 2003, Paleocology of the familiar trilobite *Elrathia*  
553 *kingii*: An early exaerobic zone inhabitant: *Geology*, v. 31, p. 941—944.

554 GOZALO, R., LIÑÁN, E., GÁMEZ VINTANED, J.A., DÍEZ ÁLVAREZ, M.E.,  
555 CHIRIVELLA MARTORELL, J.B., ZAMORA, S., ESTEVE, J. and MAYORAL, E.,  
556 2008, The Cambrian of the Cadenas Ibéricas (NE Spain) and its trilobites: *Cuadernos*  
557 *del Museo Geominero*, v. 9, p. 137—151.

558 HARPER, E.M., 2016. Uncovering the holes and cracks: from anecdote to testable  
559 hypotheses in predation studies, *Palaeontology*, v. 59, p. 597—609.

560 HARPER, E.M., PECK, L.S. and HENDRY, K.R., 2009, Patterns of shell repair in articulate  
561 brachiopods indicate size constitutes a refuge from predation: *Marine Biology*, v. 156,  
562 p. 1993—2000.

563 JAGO, J.B., GARCÍA-BELLIDO, D.C, and GEHLING, J.G., 2016, An early Cambrian  
564 chelicerate from the Emu Bay Shale, South Australia: *Palaeontology* v. 59, p. 549—  
565 562.

566 KELLEY, P.H., 1989. Evolutionary trends within bivalve prey of Chesapeake Group naticid  
567 gastropods: *Historical Biology*, v. 2, p. 139—156.

568 KELLY, P.H., KOWALEWSKI, M., and HANSEN, T.A., 2003, *Predator—Prey Interactions*  
569 *in the Fossil Record*: Kluwer Academic, New York, p. 455.

570 KIMMIG, J. and STROTZ, L.C., 2017, Coprolites in mid-Cambrian (Series 2-3) Burgess  
571 Shale-type deposits of Nevada and Utah and their ecological implications, *Bulletin of*  
572 *Geosciences*, v. 92, p. 297—309.

573 KLOMPMAKER, A.A. and KELLEY, P.H., 2015, Shell ornamentation as a likely  
574 exaptation: evidence from predatory drilling on Cenozoic bivalves, *Paleobiology*, v.  
575 41, p.187—201.

576 KOWALEWSKI, M., DULAI, A. and FÜRSICH, F.T., 1998, A fossil record full of holes:  
577 the Phanerozoic history of drilling predation: *Geology*, v. 26, p.1091—1094.

578 KOWALEWSKI, M., 2002, The fossil record of predation: an overview of analytical  
579 methods: *Paleontological Society Papers*, v. 8, p. 3—42.

580 LEIGHTON, L.R., 2001, New example of Devonian predatory boreholes and the influence of  
581 brachiopod spines on predator success: *Palaeogeography, Palaeoclimatology,*  
582 *Palaeoecology*, v. 165, p. 53—69.

583 LEIGHTON, L.R., 2011, Analyzing Predation from the Dawn of the Phanerozoic, *in*  
584 Laflamme, M., Schiffbauer, J.D., and Dornbos, S.Q. (eds.), *Quantifying the Evolution*  
585 *of Early Life*, Springer Netherlands, p. 73—109.

586 LOCHMAN, C., 1941, A pathologic pygidium from the Upper Cambrian of Missouri:  
587 *Journal of Paleontology*, v. 15, p. 324—325.

588 MCNAMARA, K. J. and TUURA, M. E., 2011, Evidence for segment polarity during  
589 regeneration in the Devonian asteropygine trilobite *Greenops widderensis*: *Journal of*  
590 *Paleontology*, v. 85, p. 106—110.



591 MERGL, M. and ZAMORA, S., 2012, New and revised occurrences of rhynchonelliformean  
592 brachiopods from the middle Cambrian of the Iberian Chains, NE Spain: Bulletin of  
593 Geosciences, v. 87, p. 571—586.

594 MORZADEC, P., 1988, Le genre *Psychopyge* (Trilobita) dans le Dévonien inférieur du Nord  
595 de l'Afrique et l'Ouest de l'Europe: Palaeontographica Abteilung A, v. 200, p. 153—  
596 161.

597 MURTAUGH, P.A., 1981, Inferring properties of mysid predation from injuries to *Daphnia*:  
598 Limnology and Oceanography, v. 26, p. 811—821.

599 NEDIN, C., 1999, *Anomalocaris* predation on nonmineralized and mineralized trilobites:  
600 Geology, v. 27, p. 987—990.

601 NETO DE CARVALHO, C., COUTO, H., FIGUEIREDO, M. V. and BAUCON, A., 2016,  
602 Estruturas biogénicas com relação microbiana nas ardósias Ordovícico Médio de  
603 Canelas (Norte de Portugal): Comunicações Geológicas, v. 103, Especial 1, p. 23—  
604 38.

605 OWEN, A.W., 1985, Trilobite abnormalities: Transactions of the Royal Society of  
606 Edinburgh: Earth Sciences, v. 76, p. 255—272.

607 PRADO, M.C., VERNEUIL, E. and BARRANDE, J., 1860, Sur l'existence de la faune  
608 primordial dans la Charne Cantabrique: Bulletin de la Société Géologique de France,  
609 Series 2, v. 17, p. 516—542.

610 PRATT, B.R., 1998, Probable predation on upper Cambrian trilobites and its relevance for  
611 the extinction of soft-bodied Burgess Shale-type animals: Lethaia, v. 31, p. 73—88.

612 R CORE TEAM, 2017, R: A language and environment for statistical computing: R  
613 Foundation for Statistical Computing, Vienna, Austria. <http://www.R-project.org/>.

- 614 ROBSON, S.P. and PRATT, B.R., 2007, Predation of late Marjuman (Cambrian)  
615 linguliformean brachiopods from the Deadwood Formation of South Dakota, USA:  
616 Lethaia, v. 40, p. 19—32.
- 617 RUDKIN, D.M., 1979, Healed injuries in *Ogygopsis klotzi* (Trilobita) from the Middle  
618 Cambrian of British Columbia: Royal Ontario Museum Life Sciences Occasional  
619 Papers, v. 32, p. 1—8.
- 620 RUSTÁN, J.J., BALSEIRO, D., WAISFELD, B., FOGLIA, R.D. and VACCARI, N.E.,  
621 2011, Infaunal molting in Trilobita and escalatory responses against predation:  
622 Geology, v. 39, p. 495—498.
- 623 SÁ, A.A. and GUTIÉRREZ-MARCO, J.C., 2015, *Aroucaichnus* igen. nov. y otros  
624 icnofósiles singulares del Ordovícico del Geoparque Arouca (Portugal): Boletín de la  
625 Sociedad Geológica del Perú, v. 110, p. 8—23.
- 626 SCHMIDT-THOMÉ, M., 1973, Beiträge zur Feinstratigraphie des Unter-Kambriums in den-  
627 Iberischen Ketten (Nordost-Spanien): Geologisches Jahrbuch Reihe, Band B7, p. 3—  
628 43.
- 629 SCHMITZ, U., 1971, Stratigraphie und sedimentologie im Kambrium und Tremadoc der  
630 Westlichen Iberischen Ketten nördlich Ateca (Zaragoza), NE-Spanien: Münstersche  
631 Forschungen zur Geologie und Paläontologie, v. 22, p. 1—123.
- 632 SCHOENEMANN, B., CLARKSON, E.N. and HØYBERGET, M., 2017, Traces of an  
633 ancient immune system—how an injured arthropod survived 465 million years ago:  
634 Scientific Reports, v. 7, p. 40330.
- 635 SCHOENER, T.W., 1979, Inferring the properties of predation and other injury-producing  
636 agents from injury frequencies: Ecology, v. 60, p. 1110—1115.
- 637 SDZUY, K., 1961, Das Kambrium Spaniens. Teil II: Trilobiten: Abhandlungen der  
638 Akademie der Wissenschaften Lit Mainz Math Nat Kl, v. 7, p. 499—594.

- 639 SINCLAIR, G.W., 1947, Two examples of injury in Ordovician trilobites: *American Journal*  
640 *of Science*, v. 245, p. 250—257.
- 641 SKINNER, E.S., 2015, Taphonomy and depositional circumstances of exceptionally  
642 preserved fossils from the Kinzers Formation (Cambrian), southeastern Pennsylvania:  
643 *Palaeogeography, Palaeoclimatology, Palaeoecology*, v. 220, p. 167—192.
- 644 SPRINKLE, J., 1973, Morphology and evolution of blastozoan echinoderms: *Museum of*  
645 *Comparative Zoology Harvard University Special Publications*, Boston, p. 283.
- 646 ŠNAJDR, M., 1978, Anomalous carapaces of Bohemian paradoxid trilobites: *Sborník*  
647 *Geologických Věd Paleontologie*, v. 20, p. 7—31.
- 648 VALENZUELA, J.I., GÁMEZ, J.A., LIÑÁN, E. and SDZUY, K., 1990, Estratigrafía del  
649 Cámbrico de la región de Brea. Cadena Ibérica oriental: *Boletín de la Real Sociedad*  
650 *Española de Historia Natural (Sección Geológica)*, v. 85, p. 45—54.
- 651 VANNIER, J., 2012, Gut contents as direct indicators for trophic relationships in the  
652 Cambrian marine ecosystem: *PLoS ONE*, v. 7, p. 1—20. e52200.  
653 <https://doi.org/10.1371/journal.pone.0052200>.
- 654 VANNIER, J. and CHEN, J., 2005, Early Cambrian food chain: new evidence from fossil  
655 aggregates in the Maotianshan Shale biota, SW China: *Palaios*, v. 20, p. 3—26.
- 656 VERMEIJ, G.J., 1977, The Mesozoic marine revolution: evidence from snails, predators and  
657 grazers: *Paleobiology*, v. 3, p. 245—258.
- 658 VERMEIJ, G.J., 1982, Unsuccessful predation and evolution: *The American Naturalist*, v.  
659 120, p. 701—720.
- 660 VERMEIJ, G.J., 1987, *Evolution and Escalation: an ecological history of life*: Princeton  
661 University Press, New Jersey, p. 544.
- 662 WALCOTT, C.D., 1911, Cambrian geology and paleontology. II. Middle Cambrian  
663 Merostomata: *Smithsonian Miscellaneous Collections*, v. 57, p. 17—40.

- 664 WEBSTER, M. and HUGHES, N.C., 1999, Compaction-related deformation in Cambrian  
665 olenelloid trilobites and its implications for fossil morphometry: *Journal of*  
666 *Paleontology*, v. 73, p. 355—371.
- 667 WEBSTER, M., GAINES, R.R. and HUGHES, N.C., 2008, Microstratigraphy, trilobite  
668 biostratigraphy, and depositional environment of the “Lower Cambrian” Ruin Wash  
669 Lagerstätte, Pioche Formation, Nevada: *Palaeogeography, Palaeoclimatology,*  
670 *Palaeoecology*, v. 264, p. 100—122.
- 671 ZACAI, A., VANNIER, J. and LEROSEY-AUBRIL, R., 2015, Reconstructing the diet of a  
672 505-million-year-old arthropod: *Sidneyia inexpectans* from the Burgess Shale fauna:  
673 *Arthropod structure and development*, v. 45, p. 200—220.
- 674 ZAMORA, S., 2010, Middle Cambrian echinoderms from North Spain show echinoderms  
675 diversified earlier in Gondwana: *Geology*, v. 38, p. 507—510.
- 676 ZAMORA, S., MAYORAL, E., ESTEVE, J., GÁMEZ VINTANED, J. A. and SANTOS, A.,  
677 2011, Exoskeletal abnormalities in paradoxid trilobites from the Cambrian of Spain,  
678 and a new type of bite trace: *Bulletin of Geosciences*, v. 86, p. 665—673.
- 679 ZHU, M.-Y., VANNIER, J., ITEN, H. and ZHAO, Y.-L., 2004, Direct evidence for predation  
680 on trilobites in the Cambrian: *Proceedings of the Royal Society of London B:*  
681 *Biological Sciences*, v. 271, p. S277—S280.

682

683

#### 684 FIGURE CAPTIONS

685

- 686 FIG 1.—Map of study area. A) IC: Iberian Chains; box shows area in B; other abbreviations:  
687 BC: Betic Cordillera; CCR: Catalan Coastal Ranges; CIZ: Central Iberian Zone; CZ:  
688 Cantabrian Zone; OMZ: Ossa-Morena Zone; PY: Pyrenees; SPZ: South Portuguese Zone;

689 WALZ: West Asturian-Leonese Zone. **B**) Box from A with Purujosa, Tierga, and Mesones de  
690 Isuela marked. **C**) MI: Mesones de Iseula; MT: Minas Tierga; BJ: Barranco del Judío; CC:  
691 Las Cuevas/ Las Coronadas. **D**) Town of Purujosa with Purujosa 3 series marked; stars  
692 indicate field sites in Murero and Mansilla Formations. Key: Units increase in age from left  
693 to right, top older than bottom (see Figure 2). (Jalón Formation is older than Ribota  
694 Formation, and Embid Formation is older than Jalón Formation.)

695

696 FIG 2.—Stratigraphy of the studied sections. Unit thicknesses and local lithologies at each of  
697 the three field sites are depicted. Stars mark levels where articulated trilobites were collected.  
698 Adapted from Gozalo et al. (2008), Gámez Vintaned et al. (2009), and Zamora et al. (2011).

699

700 FIG 3.—*Eccaparadoxides pradoanus* (Verneuil and Barrande in Prado et al. 1860) from the  
701 Purujosa Red Beds, Murero Formation (Cambrian Series 3, Drumian), Iberian Chains, Spain,  
702 at a number of stages of repair. **A**) MPZ 2011/6: nearly complete thorax with crescent shaped  
703 recent injury on a thoracic spine. **B**) MPZ 2012/844: slightly disarticulated specimen with  
704 two shortened thoracic spines. **C**) MPZ 2012/1009: rear of a thorax showing thoracic spine  
705 with slight regrowth of the tip. **D**) MPZ 2012/7808: near complete thorax with two shortened  
706 thoracic spines. **E**) Box from A, arrow indicates injured spine. **F**) Box from B, arrow  
707 indicates shortened spines. **G**) Box from C, arrow indicates spine beginning regrowth. **H**)  
708 Box from D, arrow indicates two nearly fully repaired spines. Scale bars: **A-D**) 10 mm, **E-H**)  
709 1 mm.

710

711 FIG 4.—*Eccaparadoxides pradoanus* (Verneuil and Barrande in Prado et al. 1860) nearly  
712 complete thorax from the Purujosa Red Beds, Murero Formation (Cambrian Series 3,  
713 Drumian), Iberian Chains, Spain, with additional spines growing from a previously injured

714 area. **A)** MPZ 2017/1088. **B)** Box from A, white arrows indicate spines fully repaired, black  
715 arrows indicate additional spines grown from previously injured area. Scale bars: **A)** = 5 mm,  
716 **B)** = 1 mm.

717

718 FIG 5.—Broken sclerites of *Eccaparadoxides pradoanus* (Verneuil and Barrande in Prado et  
719 al. 1860) from the Purujosa Red Beds and near Mesones de Isuela, Murero Formation  
720 (Cambrian Series 3, Drumian), Iberian Chains, Spain. **A)** MPZ 2017/398: hypostome with  
721 *Bicrescomanducator serratus* (Zamora et al. 2011) trace. **B)** MPZ 2017/398 curved break on  
722 posterior of cranidium. **C)** MPZ 2017/358 abiotic fracture at rear of cranidium. Arrows point  
723 to breaks. Scale bars = 5 mm.

724

725 FIG 6.—Broken sclerites of redlichiid trilobites with *Bicrescomanducator serratus* (Zamora  
726 et al. 2011) traces and abiotic breaks from the Huérmeda Formation near Minas Tierga  
727 (Cambrian Series 2, Stage 4), Iberian Chains, Spain. **A)** MPZ 2017/338: partial cranidium  
728 showing biotic (white arrow) and abiotic (black arrow) breaks. **B)** Close up of biotic break in  
729 A. **C)** MPZ 2017/349: partial cranidium showing biotic and abiotic breaks. **D)** Close up of C.  
730 *B. serratus* indicated by white arrow, abiotic break indicated by black arrow. Scale bars: A, C  
731 = 5 mm; B, D = 1 mm.

732

733 FIG 7.—Broken sclerites with *Bicrescomanducator serratus* (Zamora et al. 2011) traces from  
734 the Mansilla Formation near Purujosa (Cambrian Series 3, Stage 5), Iberian Chains, Spain. **A)**  
735 MPZ 2017/427: cranidium. **B)** MPZ 2017/431: fragmentary trilobite sclerite. **C)** MPZ  
736 2017/428: cranidium. **D)** MPZ 2017/430: fragmentary trilobite sclerite. *B. serratus* indicated  
737 by white arrows. Scale bars = 5 mm.

738

739 FIG 8.—Principal Component Analysis of *Bicrescomanducator serratus* (Zamora et al.  
740 2011) and abiotic breaks. Outline of the shapes of the breaks semilandmarked, as shown by  
741 dotted red line in **A**) and **B**). Black arrows indicate the direction of semilandmark placement.  
742 Scale bars = 5 mm.

743

744 FIG 9.—Principal Component Analysis plot of the semilandmarked breaks (same as Figure  
745 8), separating specimens by formation and by origin of the breaks. The overlap of previously  
746 described examples of *Bicrescomanducator serratus* (Zamora et al. 2011) (points with black  
747 dots) with new examples (points without black dots), shows the positive assignment of new  
748 material to the ichnotaxon. Circles: Huérmeda Formation (Spain, Cambrian Stage 4);  
749 triangles with point upwards: Mansilla Formation (Spain, Cambrian Stage 5); diamonds:  
750 Murero Formation (Spain, Cambrian Drumian); triangles with point downwards: Rabbitkettle  
751 Formation (Canada, Cambrian Drumian); squares: Stephen Formation (Canada, Cambrian,  
752 Stage 5); stars: Valongo Formation (Portugal, Ordovician Darriwilian); blue: abiotic; red:  
753 biotic.

754

755 FIG 10.—Idealized repair sequence of trilobite pleural spines, based on Figure 3. Grey lines  
756 show uninjured shape of middle spine, dotted black line shows previous stage of healing.  
757 Healing stages: **A**) Immediately after injury; **B**) Rounded spine after initial healing; **C**)  
758 Regrowth begins, with thin tip of pleural spine; **D**) Short spine; **E**) Healing complete, spine  
759 same length as uninjured spines.

760

761 TABLE CAPTIONS

762

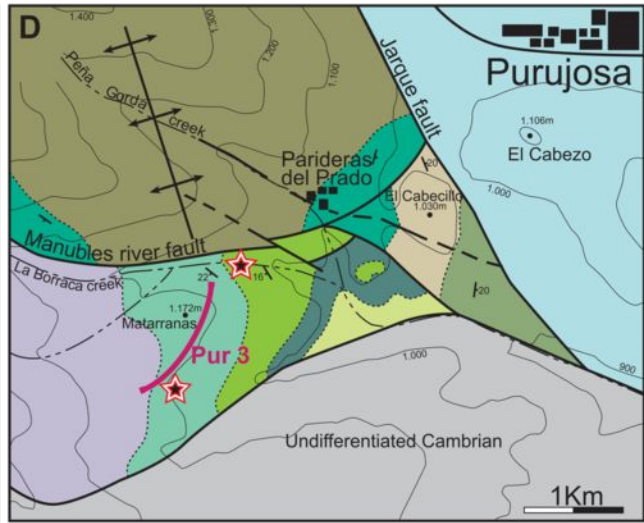
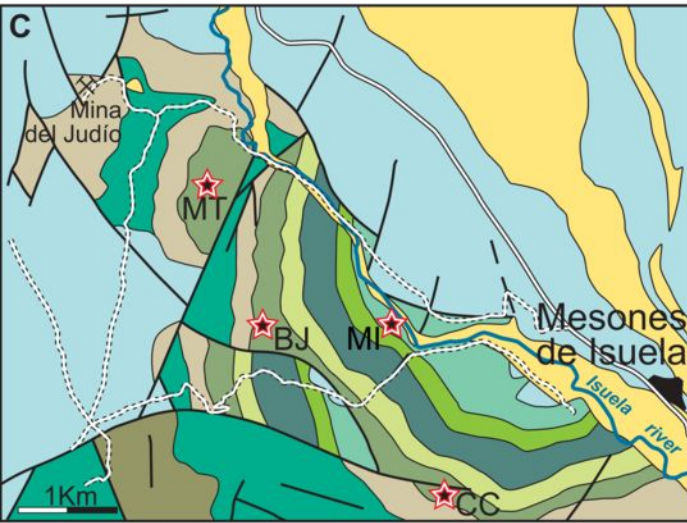
763 TABLE 1.—Frequency of repairs in Cambrian trilobites. Formation and locality information  
764 for trilobite repair frequencies and Bayesian Inference 5<sup>th</sup> and 95<sup>th</sup> percentile values. F and R  
765 are repair frequency metrics and MF is the multiple repair frequency metric (defined in  
766 methods).

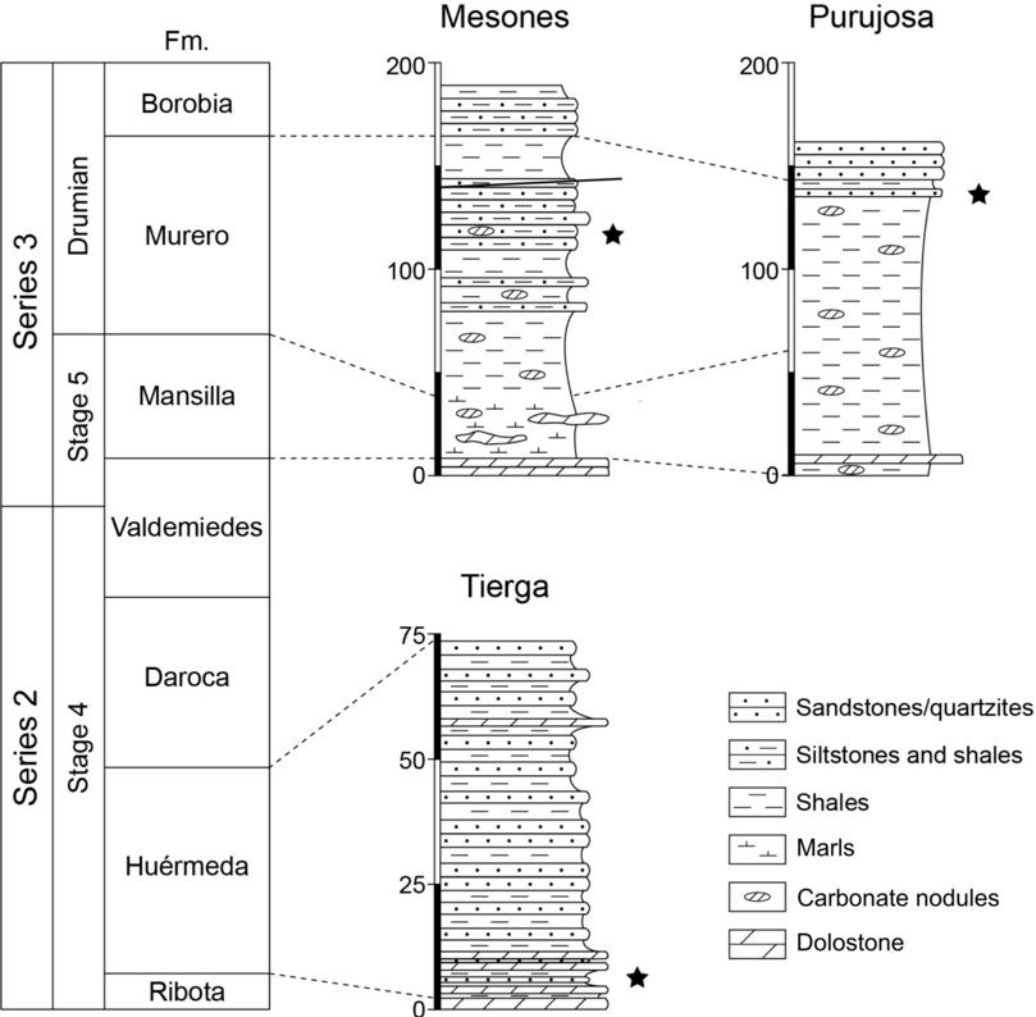
767 TABLE 2.—Adjacent injuries in complete trilobite thoraces from the Purujosa Red Beds. P-  
768 values calculated using a binomial test with 10 successes from 14 attempts. The random  
769 probability of a success (a short spine adjacent to another short spine) is 2/2207 (2 available  
770 adjacent spines, with 2207 available spines in total).

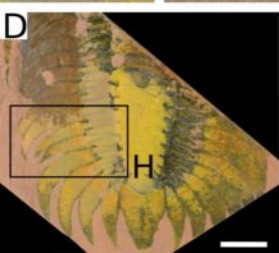
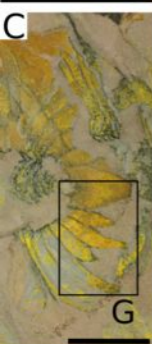
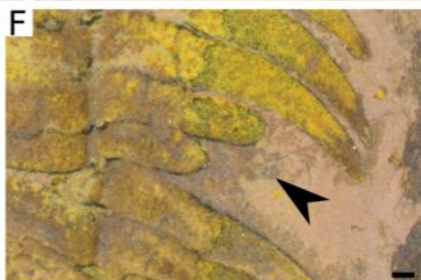
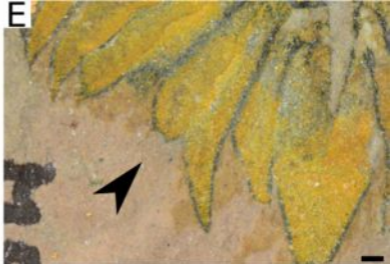
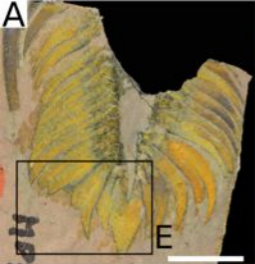
771 TABLE 3.—Analysis of the location of injuries on trilobites from the Purujosa Red Beds.  
772 Expected values calculated using a two-tailed binomial analysis. Measured values are from  
773 observations. P-values calculated as described in methods.

774

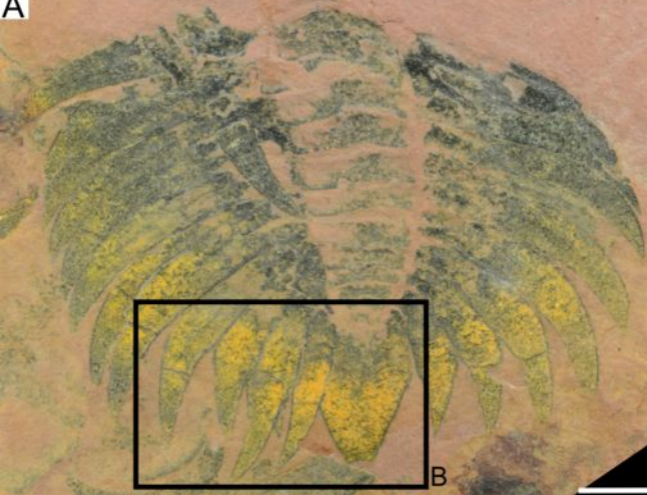




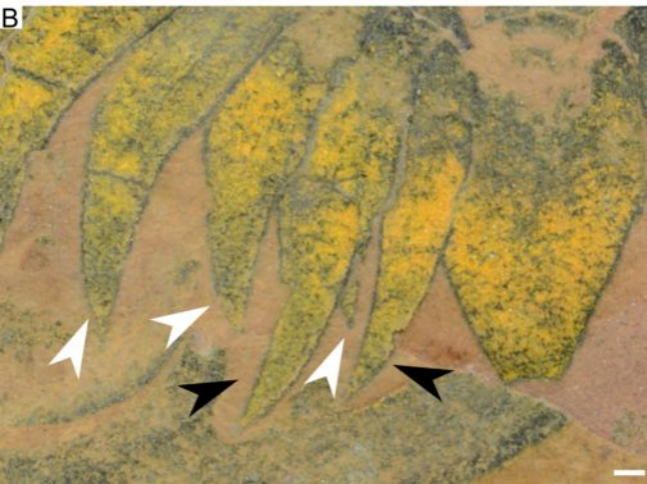


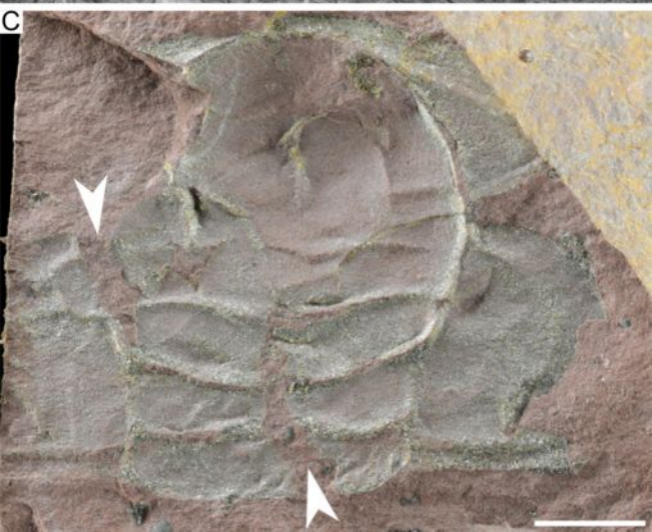
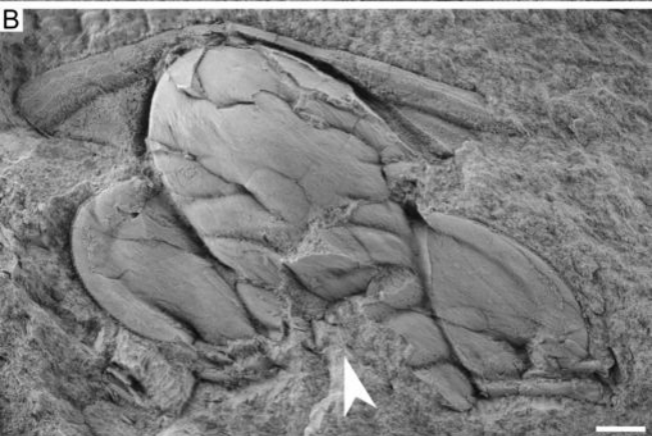
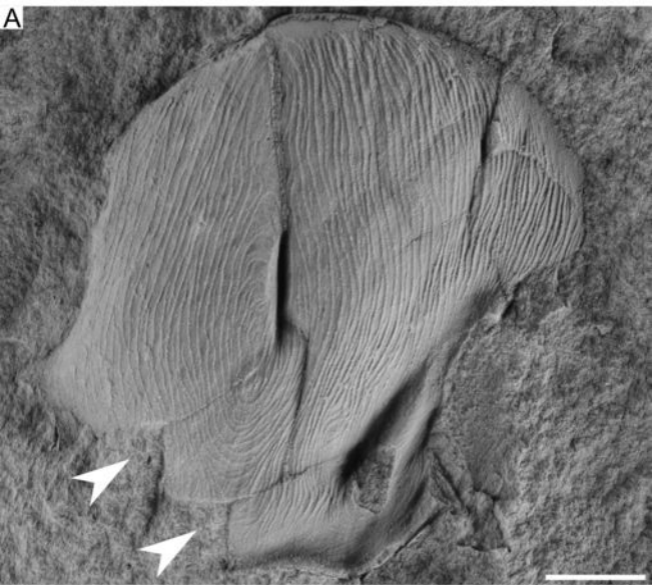


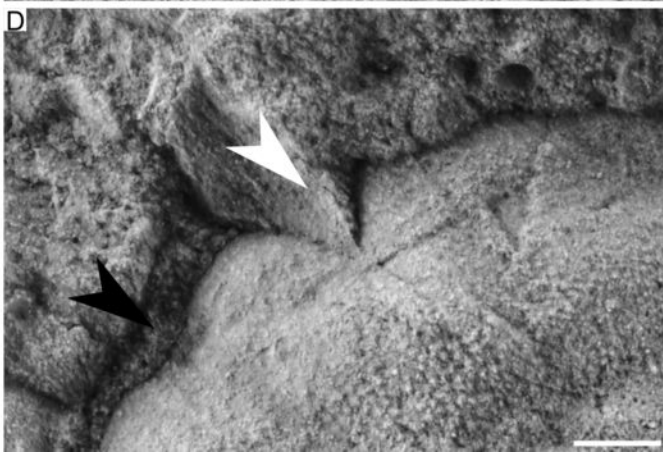
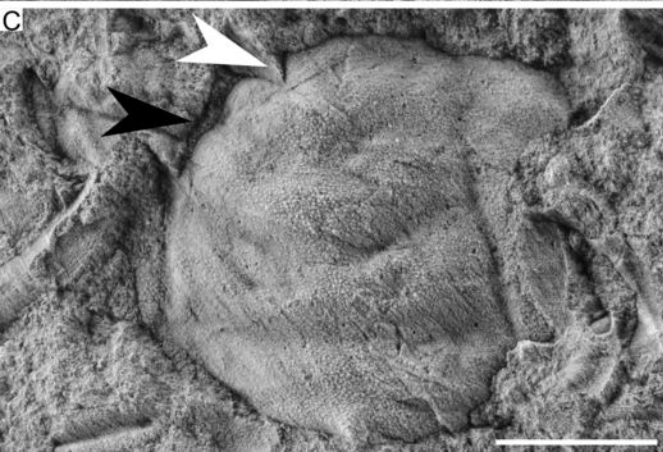
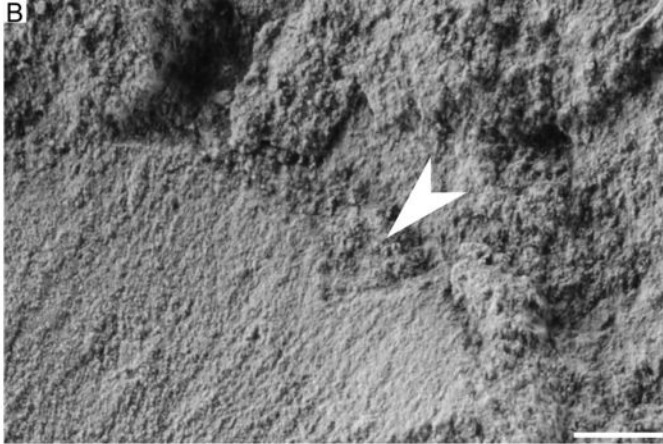
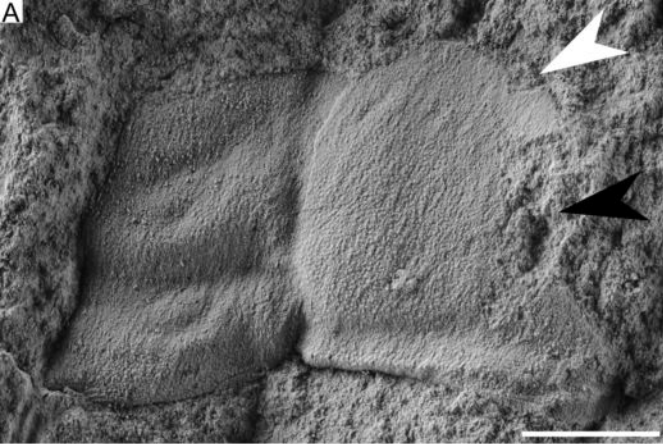
A

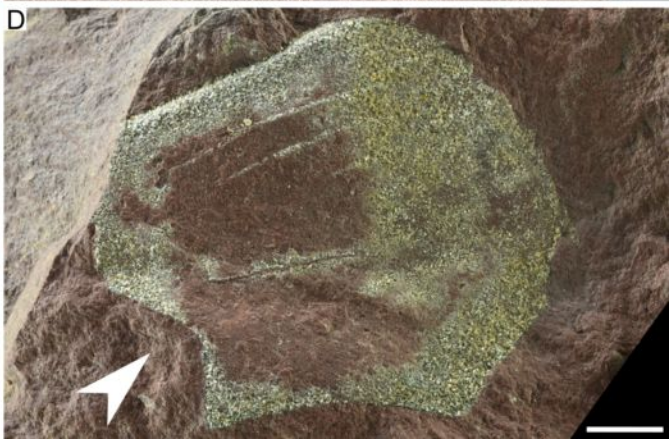
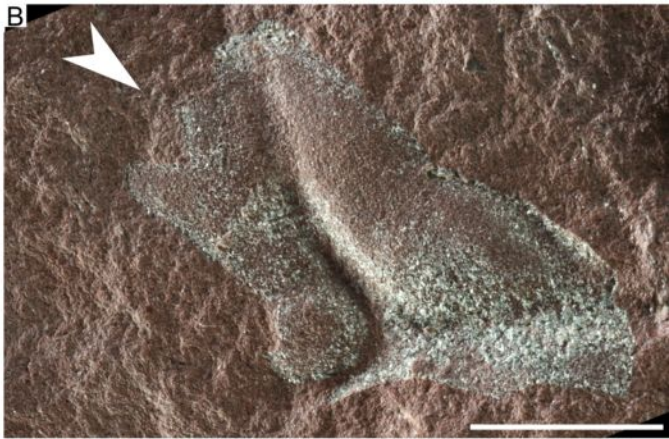
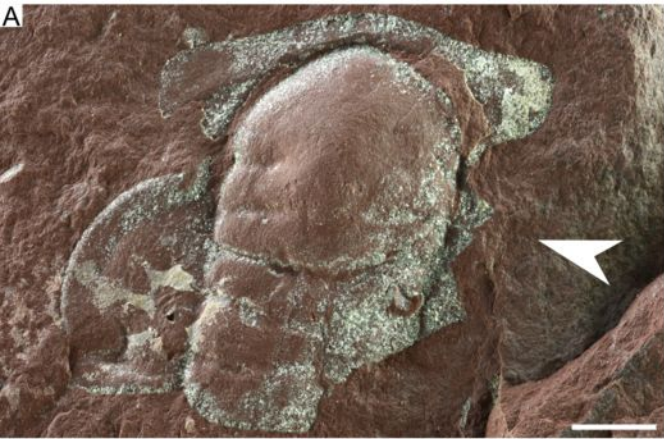


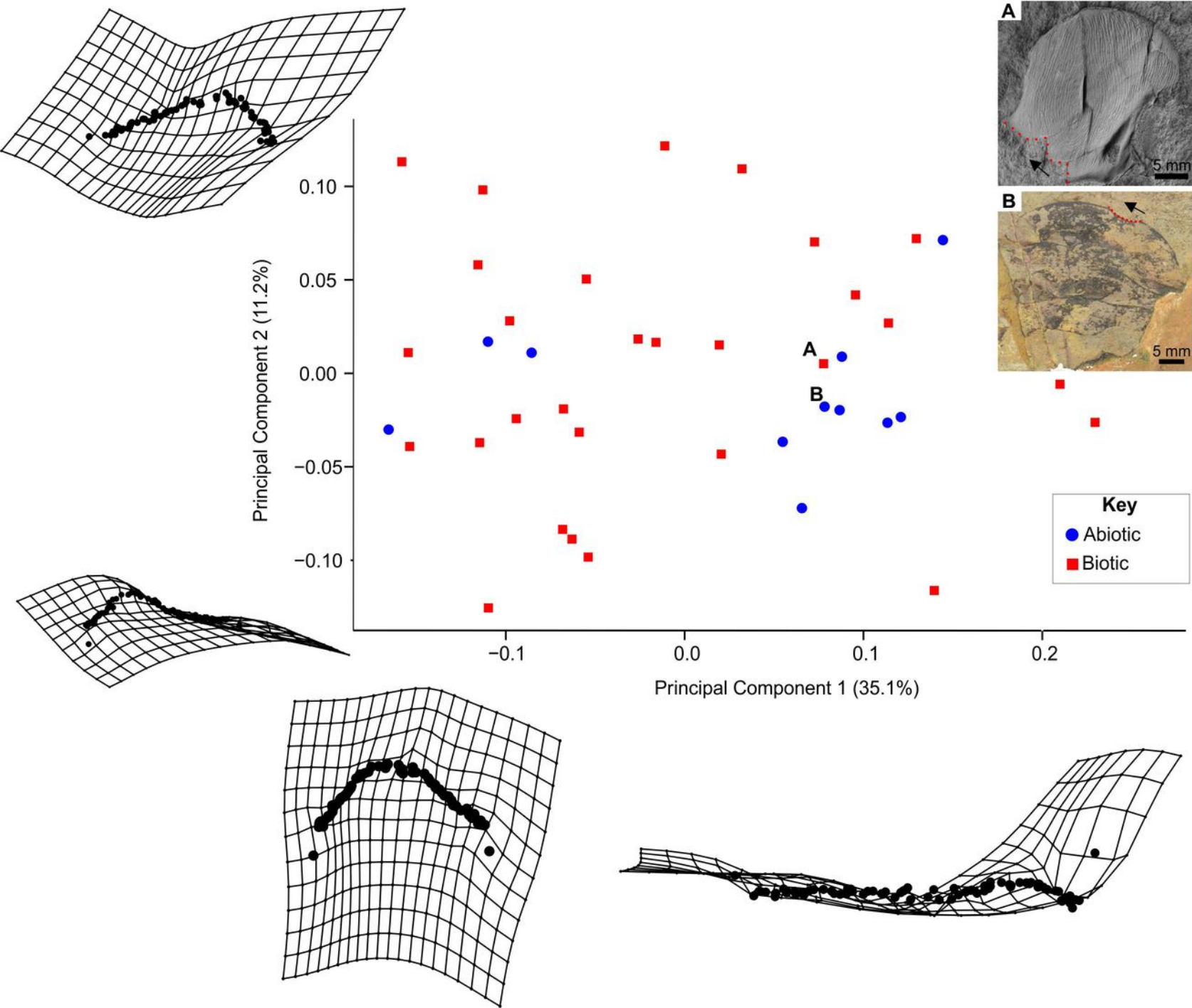
B



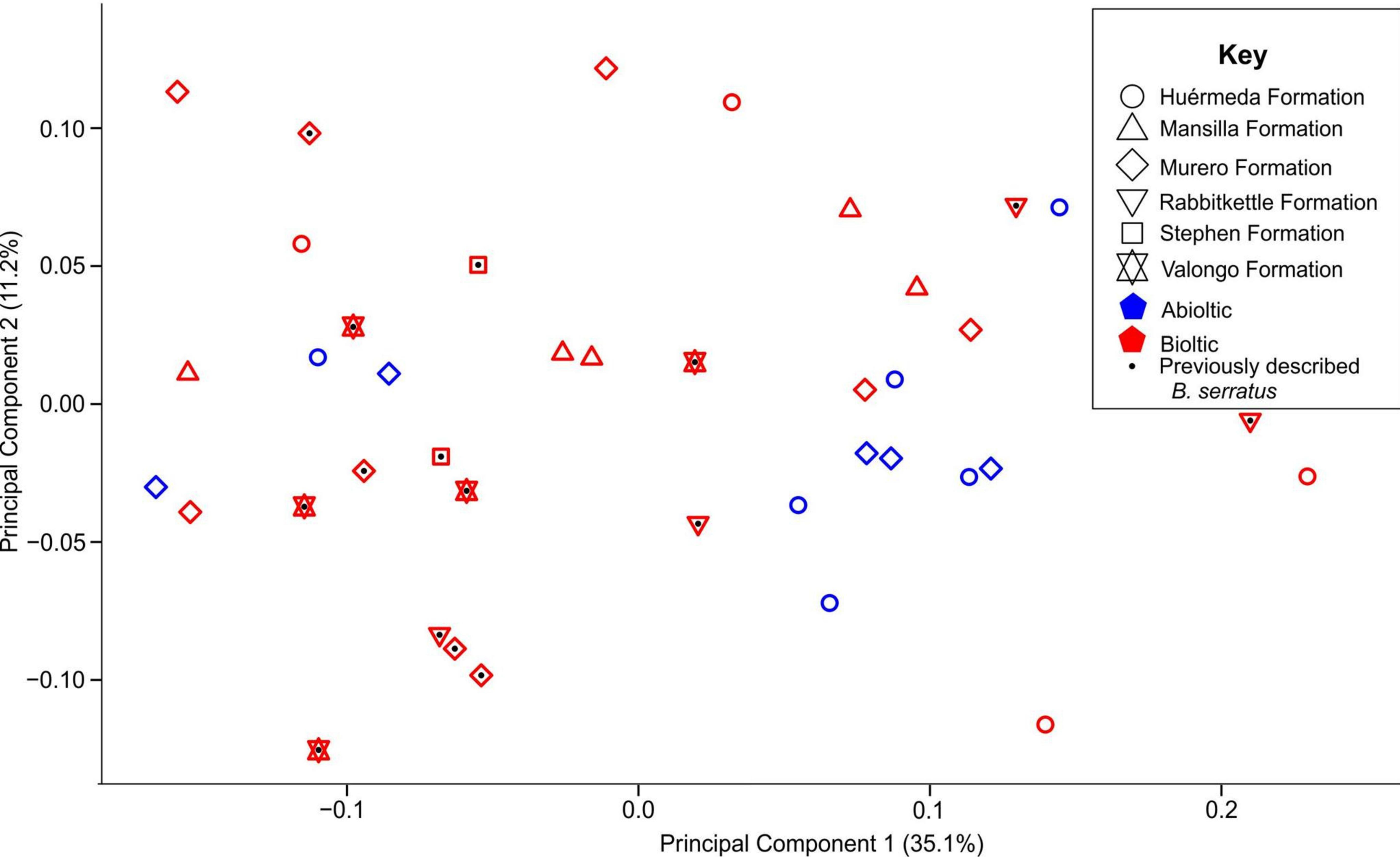












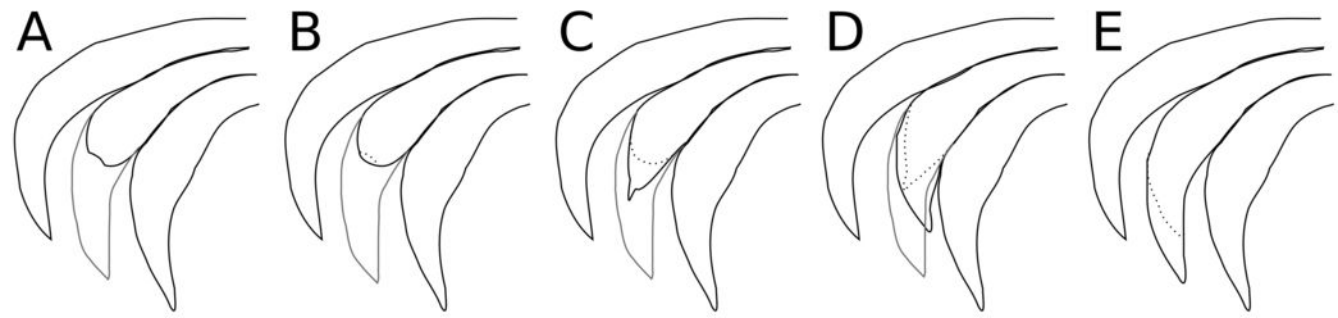


Table 1: Frequency of repairs in Cambrian trilobites

Formation/ Site	Age	Number of trilobites	Number of injured trilobites	Number of injuries	F	R	MF	F 5 <sup>th</sup> Percentile	F 95 <sup>th</sup> Percentile	R 5 <sup>th</sup> Percentile	R 95 <sup>th</sup> Percentile
Huérmeda Formation	Stage 4	45	0	0	0	0	0	0.00	0.06	0.00	0.06
Murero Formation	Drumian	97	10	12	0.11	0.09	0.20	0.08	0.19	0.06	0.17
Wheeler Formation (data from Babcock 1993)	Drumian	N/A	27	28	N/A	N/A	0.04	N/A	N/A	N/A	N/A
Minas Tierga (Huérmeda Fm)	Stage 4	30	0	0	0	0	0	0.00	0.09	0.00	0.09
Barranco del Judio (Huérmeda Fm)	Stage 4	1	0	0	0	0	0	0.02	0.78	0.02	0.78
Private collection, (Huérmeda Formation)	Stage 4	14	0	0	0	0	0	0.00	0.18	0.00	0.18
Mesones de Isuela (Murero Fm)	Drumian	23	0	0	0	0	0	0.00	0.12	0.00	0.12

Purujosa Red Beds (Murero Fm)	Drumian	69	9	10	0.14	0.13	0.11	0.09	0.23	0.08	0.21
Purujosa (other levels, from MPZ) (Murero Fm)	Drumian	5	1	2	0.4	0.2	1	0.15	0.73	0.06	0.58

Formation and locality information for trilobite repair frequencies and Bayesian Inference 5th and 95th percentile values. F and R are repair frequency metrics and MF is the multiple repair frequency metric (defined in methods).

Table 2. Adjacent injuries in complete trilobite thoraxes from Purujosa Red Beds

Number of short/injured spines	Total number of spines (assuming 32 per animal)	Number of expected injuries adjacent to another injury	Number of injured spines adjacent to injured spines	p-value
15	2208	0.013	10	$2.2 \times 10^{-16}$

P-values calculated using a binomial test with 10 successes from 14 attempts. The random probability of a success (a short spine adjacent to another short spine) is 2/2207 (2 available adjacent spines, with 2207 available spines in total).

Table 3. Location of injuries and size analysis for trilobites from Purujosa locality

Measured location of injuries		Expected location of injuries		Measured location of injuries		Expected location of injuries		2-tailed binomial p-value	
Anterior 13 thoracic segments	Posterior 3 thoracic segments	Anterior 13 thoracic segments	Posterior 3 thoracic segments	Left side of thorax	Right side of thorax	Left side of thorax	Right side of thorax	Posterior 3 thoracic segments	Left/Right side of thorax
4	6	7.3	1.7	8	8	7.5	7.5	0.0045	1
Expected values calculated using a binomial analysis. Measured values are from observations. P-values calculated as described in methods.									